Atmospheric Environment 49 (2012) 320–337

Contents lists available at SciVerse ScienceDirect

Atmospheric Environment

journal homepage: www.elsevier.com/locate/atmosenv

The model SIRANE for atmospheric urban pollutant dispersion; PART II, validation of the model on a real case study

L. Soulhac [a], P. Salizzoni [a,*], P. Mejean [a], D. Didier [b], I. Rios [c]

[a] Laboratoire de Mécanique des Fluides et d'Acoustique, UMR CNRS 5509, University of Lyon, Ecole Centrale de Lyon, INSA Lyon, Université Claude Bernard Lyon I, 36, Avenue Guy de Collongue, 69134 Ecully, France
[b] Institute of Radiation Protection and Nuclear Safety, BP 17, 92262 Fontenay-aux-Roses, France
[c] GIE ATMO-Rhône-Alpes, 3 allée des Sorbiers, 69500 Bron, France

ARTICLE INFO

Article history:
Received 15 February 2011
Received in revised form
9 November 2011
Accepted 10 November 2011

Keywords:
Field measurement campaign
Numerical modelling
Pollutant dispersion
Urban canopy
Traffic emissions

ABSTRACT

We analyse the performance of the model SIRANE by comparing its outputs to field data measured within an urban district. SIRANE is the first urban dispersion model based on the concept of street network, and contains specific parametrical law to explicitly simulate the main transfer mechanisms within the urban canopy. The model validation is performed by means of field data collected during a 15 days measurement campaign in an urban district in Lyon, France. The campaign provided information on traffic fluxes and cars emissions, meteorological conditions, background pollution levels and pollutant concentration in different location within the district. This data set, together with complementary modelling tools needed to estimate the spatial distribution of traffic fluxes, allowed us to estimate the input data required by the model. The data set provide also the information essential to evaluate the accuracy of the model outputs.

Comparison between model predictions and field measurements was performed in two ways. By evaluate the reliability of the model in simulating the spatial distribution of the pollutant and of their time variability.

The study includes a sensitivity analysis to identify the key input parameters influencing the performance of the model, namely the emissions rates and the wind velocity. The analysis focuses only on the influence of varying input parameters in the modelling chain in the model predictions and complements the analyses provided by wind tunnel studies focussing on the parameterisation implemented in the model. The study also elucidates the critical role of background concentrations that represent a significant contribution to local pollution levels. The overall model performance, measured using the Chang and Hanna (2004) criteria can be considered as 'good' except for NO and some of BTX species. The results suggest that improvements of the performances on NO require testing new photochemical models, whereas the improvement on BTX could be achieved by correcting their vehicular emissions factors.

1. Introduction

The aim of this study is to validate the model SIRANE, which is presented in the first part of this study (Soulhac et al., 2011). To that purpose we analyse its performances on real case study comparing its outputs against field data.

SIRANE is an operational model for urban air pollution that adopts parametric relations in order to simulate the pollutant dispersion phenomena in the urban boundary layer and in the urban canopy (Soulhac et al., 2011) namely, the advection along the street axes, the dispersion in street intersection and the transfer of pollutant between street and the overlying atmosphere. Even adopting this simplified approach however, SIRANE needs a large input data set. To build this data set we have to confront three main problems: characterisation of the complexity of the geometry of the domain, estimate of the intensity and spatial distribution of the pollutant sources and adoption of the crucial parameters to describe the meteorological conditions.

In order to collect the information needed to define the input data set, we performed a 2-weeks field measurements campaign within a district of Lyon. The campaign, named LYON6, took place in the VI arrondissement of Lyon, France, and provided direct

* Corresponding author. Tel.: +33 4 72186507.
E-mail addresses: pietro.salizzoni@polito.it, pietro.salizzoni@ec-lyon.fr (P. Salizzoni).

1352-2310/$ – see front matter © 2011 Elsevier Ltd. All rights reserved.
doi:10.1016/j.atmosenv.2011.11.031

measurements of traffic fluxes, meteorological conditions, pollutant concentration within the district and background pollution data. Measurements of pollutant concentration were performed in several location within the studied area, including street canyons with different aspect ratios and internal courtyard.

In the last years much efforts has been put in collecting detailed data in the urban environment to build reliable data sets for model validation. We cite here the experiment performed during the VALIUM project, in a street canyon in Hamburg (Schatzmann et al., 2005), and those performed in Central London within the DAPPLE site (Arnold et al., 2004; Wood et al., 2009). In both cases pollutant dispersion was studied by injecting a tracer gas, which allowed the control of the position and the intensity of the pollutant sources. This represents the main difference between these experiments and the LYON6 campaign, where concentration measurement concerned only car emission pollutants. A higher degree of uncertainty characterizes therefore the input parameters of our data set compared to that of provided by the cited open field gas tracer experiments.

The intensity of car emissions was estimated by merging the information provided by direct measurement and simulations of traffic fluxes within the district. Therefore the validation process presented here does not concern uniquely the performances of the model SIRANE but also those of a modelling chain (Borrego et al., 2003), given by the coupling of a dispersion model (SIRANE), a traffic model (DAVIUS) and a methodology for the estimates of the pollutant emission factors (COPERT).

Several validation studies of urban pollutant dispersion models were performed in the last years with a similar approach. This is the case for the ADMS-Urban model, whose performances were widely evaluated against field measurements over the London area (Carruthers et al., 2003). Intercomparisons between different urban dispersion models were performed by Vardoulakis et al. (2002) and more recently by Gualtieri (2010). A review of the validations of the OSPM model is given in Kakosimos et al. (2011).

The comparison between SIRANE and LYON6 data has been performed in three steps. Firstly we define the simulation scenario from the set of the measured parameters (§ 3). Secondly (§ 4) the simulation outputs are compared to the LYON6 data. Finally, (§ 5) we perform a sensitivity study in order to estimate the influence of the different input parameters on the performances of SIRANE. The statistical parameters used for the comparison are those suggested by the commonly used 'BOOT statistics' approach (Chang and Hanna, 2004).

2. Description of the LYON6 measurement campaign

The LYON6 campaign took place from July 9–24th July 2001 in the 6th arrondissement of Lyon, France (Soulhac et al., 2001). The district was chosen because of its regular geometrical characteristics, and because it was previously used for preliminary tests for SIRANE (Soulhac, 2000). The meteorological conditions were less sunny than a typical July, with the exception of the last days of the campaign. Figs. 1 and 2 show the location of the different measurements sites during the LYON6 campaign.

The measurement campaign was managed by COPARLY, the local authority for traffic and air pollution management. This was achieved by using monitoring stations for traffic, pollution and meteorological conditions. The meteorological data set was complemented by meteorological data collected at the Bron Airport.

2.1. Traffic measurements

The aim of the traffic measurements is to estimate the amount of vehicular pollutant emissions. Pneumatic car counting was placed

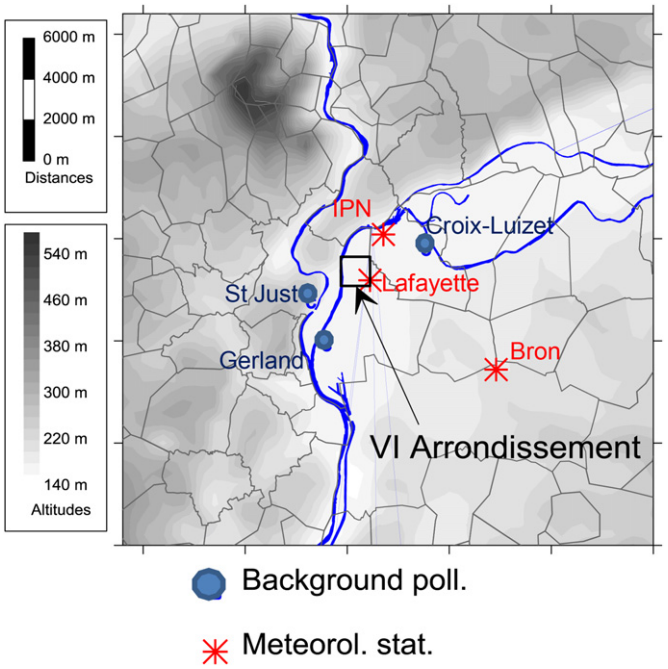

Fig. 1. Measurement locations in the LYON6 campaign in the urban agglomeration of Lyon.

in 10 streets of the district (Fig. 2). These provided a direct measurement of circulating cars each 15 min. The characteristics of the measured traffic fluxes of the ten different sites are summarised in Table 1. The goal of this measurement campaign was to collect data both from busy streets, e.g. rue Garibaldi (22,692 veh/day), and quieter streets, such us rue Tête d'Or (4110 veh/day).

The temporal evolution of the traffic, shown in Fig. 3 for rue Garibaldi, clearly shows the modulation of the fluxes during the day, with morning and evening rush hours. Fig. 3 also shows the weekly change of the fluxes, with reduced values during the weekend. These data will be used as a reference in § 3.2.1 to define weekly and daily modulation curves for traffic fluxes.

2.2. Meteorological measurements

One of the main difficulties of meteorological measurement is to collect data representative of the air circulation over the whole

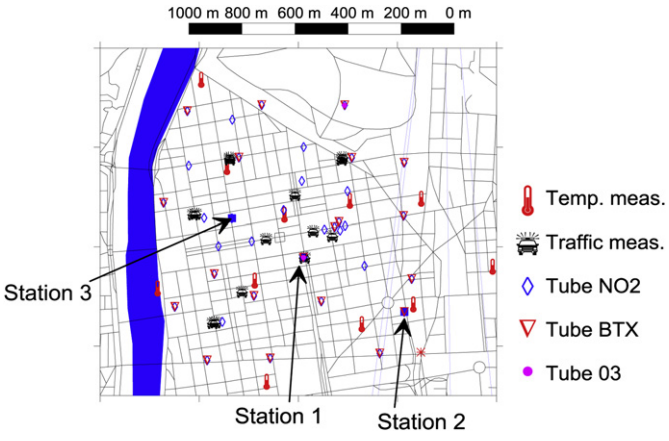

Fig. 2. Measurement locations in the LYON6 campaign within the studied district.

Table 1
Characteristics of the measured traffic fluxes in the different sites.

Measurement station	Belges	Belges (bus)	Créqui	Duquesne (east–west)	Duquesne (west→east)	Foch	Foch (bus)	Garibaldi (Sèze- Bossuet)	Garibaldi (Sully-Crillon)	Roosevelt	Saxe	Saxe (bus)	Tête d'Or	Vitton
Veh/day (15 day average)	20,826	293	4415	10,655	10,859	12,660	522	22,692	15,615	10,813	14,314	376	4110	14,597
Hourly Max (Veh/h)	2330	39	656	1224	1287	1483	114	2560	1820	1124	1571	66	562	1600
15 min Max	621	14	196	331	345	441	44	671	484	318	468	26	161	437

urban district. Two choices are available: collect the meteorological data by means of a monitoring station placed within the district or outside of it, in open terrain regions in the surrounding areas. Both choices can be critical. In the first case the measurements are performed in a built environment and can therefore be influenced by local effects such as building wakes and shadows. In the second case, although the data are certainly not affected by local effect, some of the measured parameters may not be representative of the meteorological conditions in the district. This can be the case for example for the wind velocity, whose vertical profile in a sub-urban area may be significantly altered by the increased drag exerted by the high building density of a city. In this latter case a corrective procedure must be applied in order to use the data collected outside of the district to characterise the meteorological conditions over it (§ 3.3).

In the present study the meteorological measurements were performed by 3 stations (Fig. 1), one outside the urban area and two within it. The station outside the urban area was located at the Bron Airport, at about 7 km from the studied district, and placed away from any building that could have a direct influence on the measurements. The wind speed and direction was measured with a cup anemometer and a wind vane placed at 10 m from the ground. The other measured parameters were the ground level temperature and humidity, the cloud coverage and the precipitation intensity.

The two other stations were placed within the Lyon urban area. These are referred to as the station 'Lafayette' and 'IPN'. The Station 'Lafayette' is the only one placed within the studied district and was equipped with a cup anemometer and a wind vane e thermometer and a hygrometer. The 'IPN' station was specifically installed for this campaign at about 1.5 km from the studied district with a sonic anemometer, providing measurements of the three wind velocity component and of the air temperature. The instruments were positioned above a building at about 10 m from the roof level. It is worth noting that in both cases the sensor were placed within the urban roughness sub-layer and we cannot exclude the influence of local effect on the measured parameters, in particular on the wind speed and direction. The meteorological data set is completed by temperature measurements performed in several places within the district (Fig. 2). All parameters have been measured at an hourly frequency.

2.3. Pollution measurements

The purpose of the pollution measurements is to determine the hourly evolution of traffic induced pollutant concentration in the streets of the district. The measurements concerned the following chemical species: nitrogen oxides, ozone and volatile organic compounds (mainly benzene, toluene and xylem) and were performed with two different measurement systems:

- *Analysers placed in monitoring stations*: three measurement stations of the COPARLY monitoring network (Fig. 2), referred to as Station 1, Station 2 and Station 3, were placed within the studied district and provided hourly concentrations. Station 1 was placed in a street canyon with a high intensity of traffic (Rue Garibaldi). The analyser was placed at 2 m from the ground at few centimetres from a building wall, therefore in a region where the concentration gradients are expected to be small compared to other region within the canyon. Station 2 and Station 3 were placed in internal school courts, without any pollutant source in it, within which the pollutant concentrations are expected to be almost homogeneous. Even in these cases the analysers were placed at 2 m from the ground level. Other stations placed outside the district were used to estimate the background pollutant concentration levels (Fig. 1).
- *Passive diffusion tubes (PDT)*: the pollutant measurements were complemented by 60 standard PDT which were placed within the studied urban district (Fig. 2), providing pollutant concentrations averaged over 15 days, i.e. the whole campaign duration. Some of the tubes were placed close together in order to evaluate their measurement errors. Part of them were also placed close to the existing monitoring stations in order to obtain an estimate of the relative measurement error compared to the measurements provided by the analyser.

The cartography of the pollution levels averaged over a period of 15 days and measured by the diffusion tubes is shown in Fig. 4. The levels of NO_2 and BTX over the district show high spatial variability.

Table 2 shows the differences registered between 10 tubes placed at the same location and the differences between measurements by the 10 tubes and the analysers placed nearby monitoring network station. Differences between the tubes placed

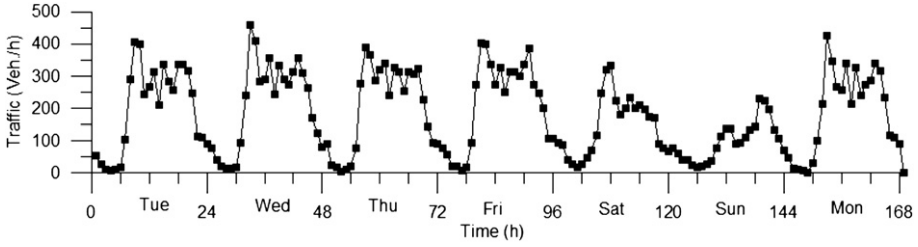

Fig. 3. Traffic measurements in rue Garibaldi from Tuesday the 3rd July at midnight to Monday the 9th July at 23 h (local hour).

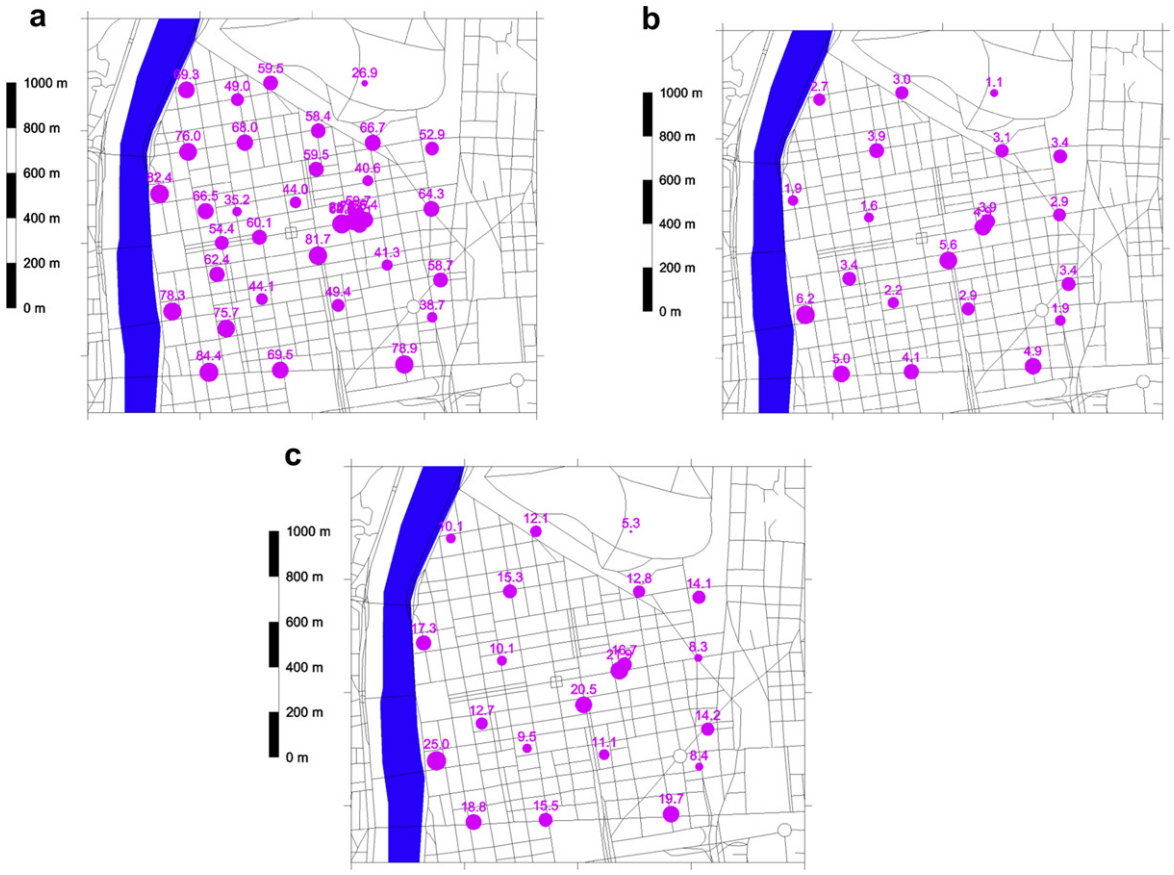

Fig. 4. Pollution cartography obtained by passive diffusion tubes (concentrations averaged over 15 days expressed in $\mu g/m^3$). a) NO_2; b) benzene; c) toluene.

at a same location are slight for NO_2, benzene, toluene and m-xylem (less than 6%) and higher for all other BTX. Conversely, the relative errors between tubes and measurements given by the monitoring stations are significant (Table 2). However, as shown Fig. 5, the tubes and analysers measurements are highly correlated to each other ($R^2 = 0.99$), with a systematic overestimation of the PDT (the slope of the linear regression is 0.69). This high correlation, together with the small differences registered in different PDT, suggests that the PDT measurements are biased by a systematic error which is independent of the chemical species of the pollutant considered. This kind of overestimation by PDT have been extensively analysed in previous studies (Campbell et al., 1994; Gair and Penkett, 1995; Heal et al., 1999). In particular Gair and Penkett (1995) have shown that standard PDT with a tube of 7.1 cm length and with a 1.2 cm diameter can be subjected to systematic errors due to a shortening of the effective diffusion length caused by air velocity across the face of the tube. This effect, that induces overestimations up to 40%, can be considered as a plausible explanation of the systematic differences between PDT and analysers registered in our measurements campaign.

Summarising, the PDT measurements show slight differences to each other and a significant systematic difference with the analysers. For these reasons we have assumed that the PDT measurements were reliable in order to quantify the spatial variability of the pollutant. However, in order to compare these measurements to the SIRANE outputs, we have corrected the PDT concentrations by a factor 0.69, i.e. the slope of the linear regression in Fig. 5.

3. Definition of the simulation scenario and model set-up

The definition of the simulation scenario implies the management of all data acquired by the field measurements (within and

Table 2
Relative difference between measurements performed by monitoring stations and passive diffusion tubes.

	NO_2 Station 3	NO_2 Garibaldi	Benzène Garibaldi	Toluène Garibaldi	Ethylbenze Garibaldi	p-Xylem Garibaldi	m-Xylem Garibaldi	o-Xylem Garibaldi
Ensemble average over 10 tubes ($\mu g/m^3$)	35.2	81.7	5.6	20.5	7.4	5.3	13.7	4.9
Standard deviation of 10 tubes ($\mu g/m^3$)	0.7	1.6	0.3	1.1	1.3	0.8	0.8	1.7
Standard deviation/mean (%)	2.1	2	4.9	5.3	18.3	15.3	5.9	34.6
Time average of the analyser ($\mu g/m^3$)	26	56	5	17				
Relative difference between PDT and analysers	35.5	45.8	11.4	20.6				

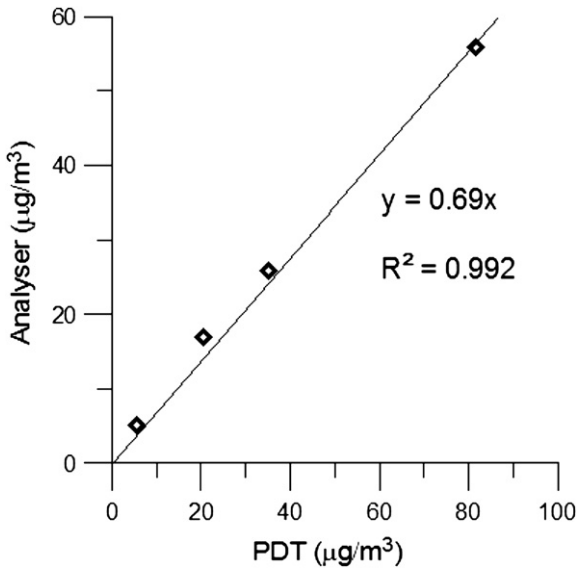

Fig. 5. Correlation between PDT and analyser concentration measurements.

outside the studied district) which are necessary to run SIRANE. This encompasses the urban geometry, the spatial and temporal distribution of pollutant emissions, the temporal evolution of the meteorological parameters and of the background pollution (Fig. 6).

3.1. Urban geometry

SIRANE represents a district as a street network, made up of arcs – representing streets – and nodes – representing intersections (Soulhac et al., 2011). Each street is modelled as a cavity of rectangular cross section, referred to as a street canyon, characterised by a width W, a height H, and a length L, that were computed from detailed information supplied by a GIS dataset of (Fig. 7). A distributed surface roughness $z_{0,build}$ on the street canyon walls models the influence of smaller scale elements and its value is assumed to be equal to 0.05 m. The computation of the streets dimensions was performed by means of a specific numerical tool, which is presented in Soulhac et al. (2011). The urban data processing allows 'narrow' ($H/W > 1/3$) and 'wide' ($H/W < 1/3$) streets to be distinguished. A narrow street is characterized by the so called 'street-canyon' effect, i.e. the pollutant retention within the street volume by the recirculating air motion within it. In the present case the simulation domain comprises the whole 6th arrondissement in Lyon, which extend for about 1.6 km in the E-W direction and 1.6 km in the N–S direction (Fig. 1). The district includes 491 street segments, 400 of which are street canyons.

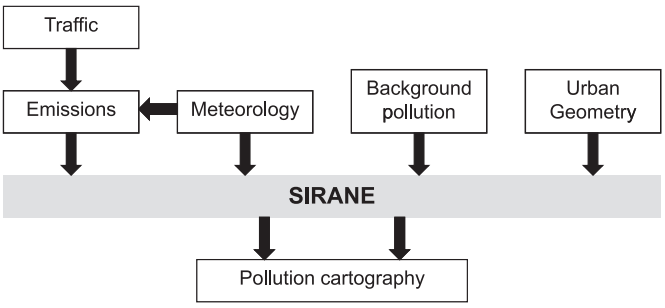

Fig. 6. Scheme of input data for SIRANE.

3.2. Traffic and emission data

We consider only the contribution of cars and neglect any other possible source. This choice is justified by the absence of any light or heavy industry within the studied district. Furthermore, since the measurement period was in July, there was no domestic heating contributing to air pollution. To simulate traffic emissions, we first estimate the mean traffic flow rate in each street of the district and subsequently compute their emission.

3.2.1. Traffic scenario

To define the hourly evolution of traffic fluxes over the district, we posses two types of information:

- The hourly traffic count performed in 10 streets during the LYON6 campaign.
- Traffic simulations at rush hours in the main streets of the whole urban area of Lyon performed with the software DAVISUM (Friedrich, 1999; Fellendorf et al., 2000) by the Grand Lyon authority. These refer to standard daily rush hours (in the morning and in the evening), without any direct correlation with the LYON6 campaign.

In order to obtain the information required to run SIRANE we had to merge the information provided by the traffic simulation and those provided by direct traffic measurements (Fig. 3). This was done by applying a modulation curve inferred by direct measurements, which gives information on the temporal evolution of traffic fluxes, to the rush hour data provided by DAVISUM, which gives the spatial distribution of traffic fluxes.

The modulation curve was assumed to be homogeneous over the whole district, even if the curves obtained by the direct observation in the 10 different measurement points did show differences one from the other. To obtain a unique modulation curve for the whole district we averaged the ten different curves inferred from the 10 measurement sites. We define three types of modulation curves, one for weekdays, one for Saturday and one for Sunday (Fig. 8). The modulation coefficient are referred to as $AJ_{js,h}$, where *js* indicates the day of the week and *h* indicates the hour of the day (the average of AJ over a day is equal to 1). To take into account weekly variation of traffic fluxes we have also used a daily modulation coefficient, referred to as Am_j. Therefore the traffic flux within a street *r* is computed by the following relations:

$$\begin{aligned} Q_{r,j,h} &= Am_j \frac{AJ_{js,h}}{AJ_{2,9}} Qmorning_r \quad \text{if } h \in [0.12[\\ Q_{r,j,h} &= Am_j \frac{AJ_{js,h}}{AJ_{2,i9}} Qevening_r \quad \text{if } h \in [12.24[\end{aligned} \tag{1}$$

where Qmorning and Qevening are the matrix of the traffic distribution computed by DAVISUM at rush hours in the morning and in the evening. We have assumed that the morning rush hour took place from 8 to 9 am (local hour) on Tuesday, and that this value could be used as a reference for the modulation between midnight and noon. Similarly we have assumed that the evening rush hours corresponded to the interval 6–7 pm on Tuesday, and that this value could be used as a reference for the modulation between noon and midnight.

To test our traffic estimates we have compared, for the 10 different observation sites, the traffic simulated by relation (1) to the measured values. The comparison is performed by estimating the fractional bias and the relative error between the measured and

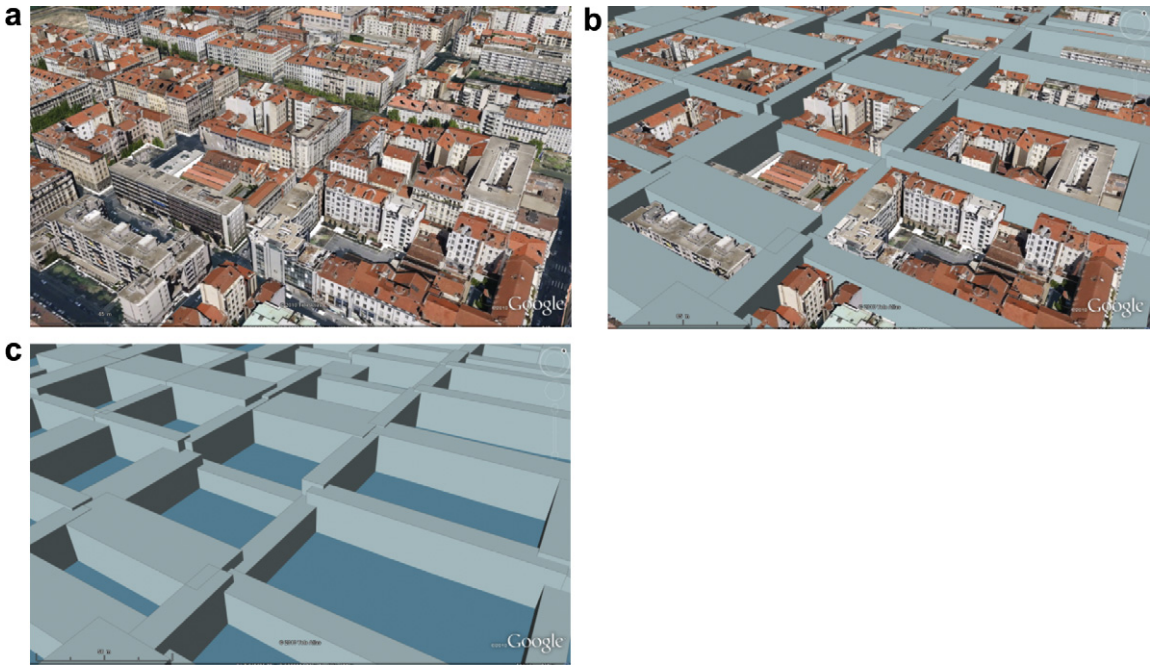

Fig. 7. Definition of the street network from GIS data of the district geometry. a) real urban geometry; b) estimation of box dimensions from GIS data; c) street network.

modelled quantities, referred to as C_p and C_m respectively, and defined as:

- The fractional bias FB $= (\overline{C_p} - \overline{C_m})/(1/2(\overline{C_p} + \overline{C_m}))$.
- The relative error: ER $= \overline{\left(\frac{|C_p - C_m|}{1/2(C_p + C_m)}\right)}$.

Results are presented in Fig. 9 and Table 3. The fractional bias between simulated and measured traffic varies between 0 and 0.35 and the mean relative deviation between 0.15 and 0.36. These results imply that at given hours, when the two effects are superposed, the total errors can exceed 50%.

To determine pollutant emissions it is also necessary to know the averaged speed of the vehicles in each street. Since direct

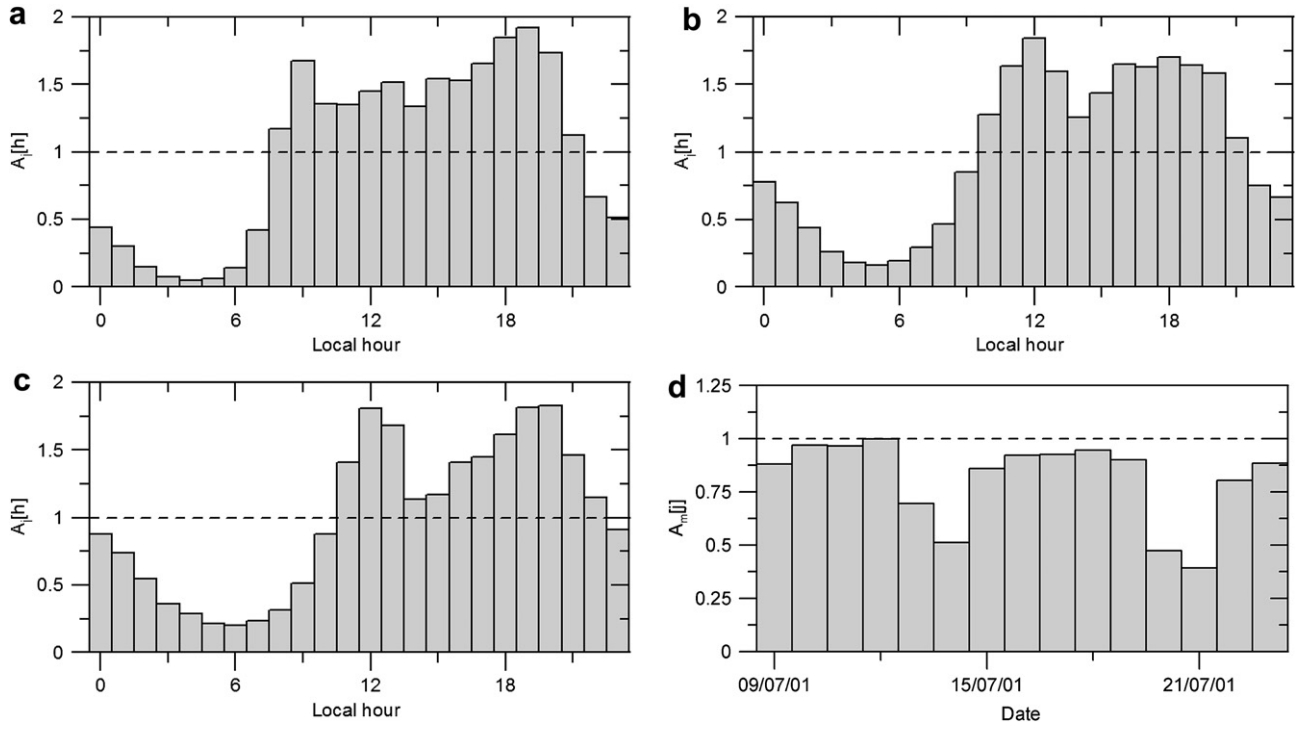

Fig. 8. Hourly and daily modulation curves for the estimate of traffic fluxes. a) hourly modulation for a day during the week; b) hourly modulation for Saturday; c) hourly modulation for Sunday; d) daily modulation for the period of the campaign LYON6.

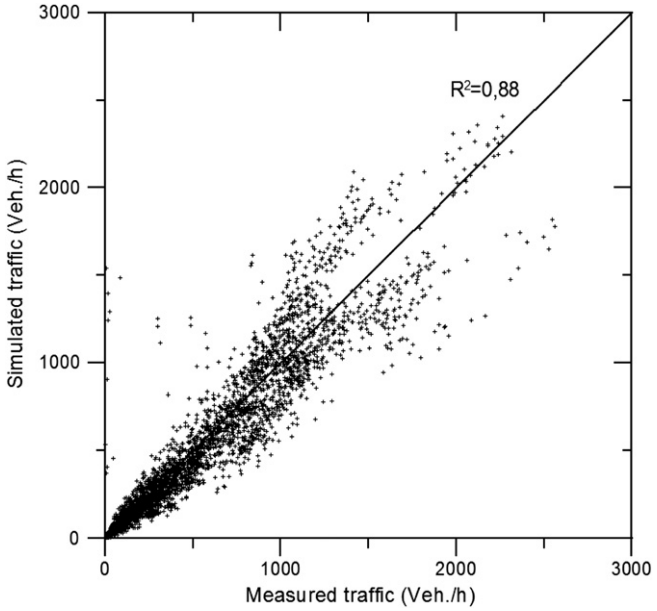

Fig. 9. Comparison between simulated and measured traffic in 10 streets of the district. Each point corresponds to an hourly averaged values.

measurement of this speed were not available, we have estimated it using the software DAVISUM, which computes it via a simple analytic relation between the street saturation rate (ratio between actual and maximal traffic flow rate) and the average speed of the vehicles:

$$V(X) = V_{\max}\frac{1.2-X}{1.2-0.3X} \text{ if } X < 0.92$$

$$V(X) = \frac{V(0.92)}{1-\frac{1}{V(0.92)}\frac{\partial V}{\partial X}\Big|_{0.92}(X-0.92)} \text{ if } 0.92 < X < 1$$

$$\text{with } X = Q/Q_{\text{sat}}$$

$$V(X) = \frac{V(1)}{X^2} \tag{2}$$

where $V_{\max}$ is the maximal speed of vehicles. The saturation flow rate Q_{sat} within each street is an input parameter of the software DAVISUM.

Finally, we list the main limitations of the methodology adopted for the estimate of traffic emissions:

- *Lack of data for secondary streets*: The simulation is performed assuming that the traffic is distributed only along the main streets of the district and neglecting the traffic in the secondary streets.
- *Traffic simulations at rush hours*: our approach is based on the estimate of traffic fluxes at rush hours. However, the spatial distribution of the traffic fluxes during the rest of the day is certainly different to that observed during the rush hours.
- *Uniform modulation of traffic flow rates over all the district*: this assumption does not necessarily match on site observations. When the total traffic volume increases approximately 50% the flow within each street is inhibited as the street approaches saturation. However, the improvement of this approach would require sophisticated unsteady traffic models.

Summarising, even if the traffic scenarios are estimated by a wide ensemble of data provided by simulations and direct measurements, the adopted methodology provides results which are affected by non negligible errors.

3.2.2. Pollutant emissions

To estimate pollutant emissions, we used the COPERT III methodology (Ntziachristos and Samaras, 2000), which adopts empirical relations to relate a vehicles emission to its speed. These relations, referred to as emission factors, are specified for the different pollutant species and 105 different vehicle classes. The emission factor also takes into account if cars are running with cold and hot engines. The estimate of the traffic emitted pollutant within a street is given by the following relation:

$$E_{\text{total}} = Q_{\text{veh.}} L_{\text{street}} \sum_i \frac{p_i}{100} e_i^{\text{hot}}(V)\left[1-\beta_i(T_{\text{air}})+\beta_i(T_{\text{air}})R_i^{\text{cold}}(V,T_{\text{air}})\right]$$

$$\text{with} \begin{cases} E_{\text{total}} = \text{total emission of pollutant within the street [kg/s]} \\ Q_{\text{veh.}} = \text{vehicular flux in a street [veh./s]} \\ L_{\text{street}} = \text{street lenght [m]} \\ p_i = \text{percentage of } i \text{ type vehicles [\%]} \\ e_i^{\text{hot}}(V) = \text{hot emission factor for } i \text{ type vehicles [kg/m]} \\ \beta_i(T_{\text{air}}) = \text{Fraction of traffic flux with cold engine } i\,[-] \\ R_i^{\text{cold}}(V,T_{\text{air}}) = \text{cold emission rate for } i \text{ type vehicles } [-] \\ V = \text{Vehicles average speed [km/h]} \\ T_{\text{air}} = \text{air temperature } [^\circ\text{C}] \end{cases} \tag{3}$$

The parameters Q_{veh} and V have been deduced from traffic scenarios for each street (§ 3.2.1). The air temperature is that measured hourly at the meteorological station Lafayette (§ 3.3). The average distance run with a 'cold' engine, required to estimate the coefficient β_i, has been assumed to be 12 km (value recommended by Ntziachristos and Samaras, 2000). The coefficients p_i related to the percentage of the composition of the vehicular fleet has been determined according to literature data (Bourdeau, 1997) and assuming 6 vehicle categories (See Table 4).

The emissions of different species of volatile organic compounds (VOC) were estimated adopting the methodology COPERT III, which provides distribution coefficients to apply to the total amount of

Table 3
Comparison between simulated and measured traffic in 10 streets of the district.

Site	Fractional Bias	Relative error
Belges	0.23	0.209
Créqui	0.101	0.319
Duquesne (est→west)	0.046	0.153
Duquesne (west→est)	0.183	0.360
Foch	0.075	0.164
Garibaldi (Sèze-Bossuet)	0.165	0.231
Garibaldi (Sully-Crillon)	0.0002	0.179
Roosevelt	0.346	0.188
Saxe	0.060	0.157
Tête d'Or	0.195	0.292
Vitton	0.237	0.189
Mean	0.149	0.222

Table 4
Composition of the vehicular fleet.

Vehicle type	p_i coefficient (Bourdeau, 1997)
Private cars (VP)	0.7238
Light utility vehicles (LUV)	0.1492
Heavy goods vehicles (HGV)	0.909
Public transport buses	0.0061
Coaches	0
Motorcycles	0.03
Total	1

Table 5
VOC speciation matrix, percentages of the total mass of VOC.

Pollutant	Fuel cars		PV and LUV	Diesel HGV	GPL Vehicles
	Conventional	Euro I to IV			
Benzene	6.83%	5.61%	1.98%	0.07%	0.63%
Toluene	12.84%	10.98%	0.69%	0.01%	1.22%
mp-Xylem	6.66%	5.43%	0.61%	0.98%	0.75%
o-Xylem	4.52%	2.26%	0.27%	0.40%	0.26%

VOC. The coefficients related to BTX are given in Table 5. In § 5.1 we discuss the errors related to these coefficients.

Using this information we determined the spatial distribution (Fig. 10) and temporal evolution (Fig. 11) of car emissions of NO_X, Benzene, Toluene, mp-Xylem ando-Xylem. Since we expect these estimate to be affected by a significant error, we have performed a sensitivity analysis on the different steps of the methodology adopted to estimate vehicle emissions (§ 5.1).

3.3. Meteorological data

In order to define the meteorological input for SIRANE we have integrated measurements performed in the three different stations, Lafayette, IPN and Bron airport.

The reference values for humidity and temperature were those registered at Lafayette stations and which were not significantly different from those measured in the 'IPN' station, the other station within the urban area. The cloud coverage and precipitation intensity were provided by the Bron station. The most critical point, as expected, was to estimate reliable values of wind speed and direction.

In its present version SIRANE assumes that the atmospheric wind field above the studied district is homogeneous in the horizontal plane and hence neglects the presence of a roughness sublayer above the building roofs. The vertical distribution of dynamical and thermo-dynamical parameters is computed according to Monin–Obhukov similarity theory (Soulhac et al., 2011) from single point measurements. It is therefore essential that the measured wind speed and direction in the surface layer are not influenced by local effects.

The plot in Fig. 12-a show that the wind directions measured in the two urban stations is affected by a significant scatter. A similar scatter was observed between the data registered at open terrain station (Bron airport) and the two urban stations (Lafayette and IPN) and can be reasonably attributed to the effects of the wakes down- wind of the buildings in the surrounding areas of the two urban stations.

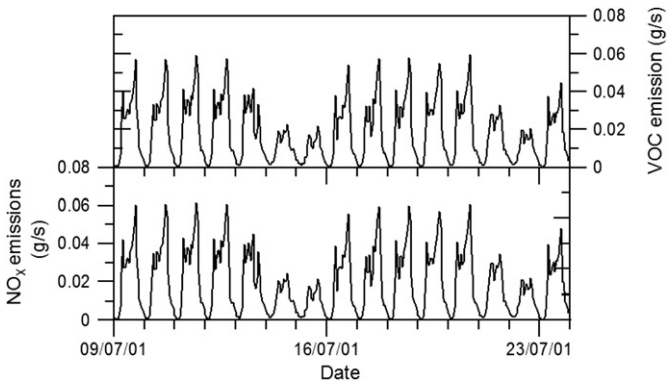

Fig. 11. Temporal evolution of NO_X (equivalent NO_2) and total COV emissions in avenue Foch.

For these reasons we have assumed that the reference direction and speed were those registered at the Bron airport. However, since the Bron Airport is placed within a sub-urban area, the measured wind speed has to be corrected before using it to describe the meteorological condition above the studied district, where the wind field is influenced by the presence of buildings. SIRANE's meteorological pre-processor allows us to apply this correction, by estimating the effect of a varying roughness length and displacement height and by assuming that the geostrophic wind at the top of the boundary layer above the two sites is identical. This is a reasonable assumption since the two sites are not too far away one from each other and since the terrain between them is flat. The characteristics of the three measurement sites are given in Table 6.

In order to validate this approach we have compared the corrected wind data registered at the Bron airport station to those measured at two urban monitoring stations Lafayette and IPN.

The wind speed given by the output of SIRANE's meteorological pre-processor agrees well (Fig. 13) with the data recorded within the district and is therefore able to simulate the increased drag effect exerted by buildings. The main limitation of this methodology is that it does not allow us to take into account any possible change in wind direction. Since the wind field is almost unperturbed by topographic effect, we would expect these deviations to

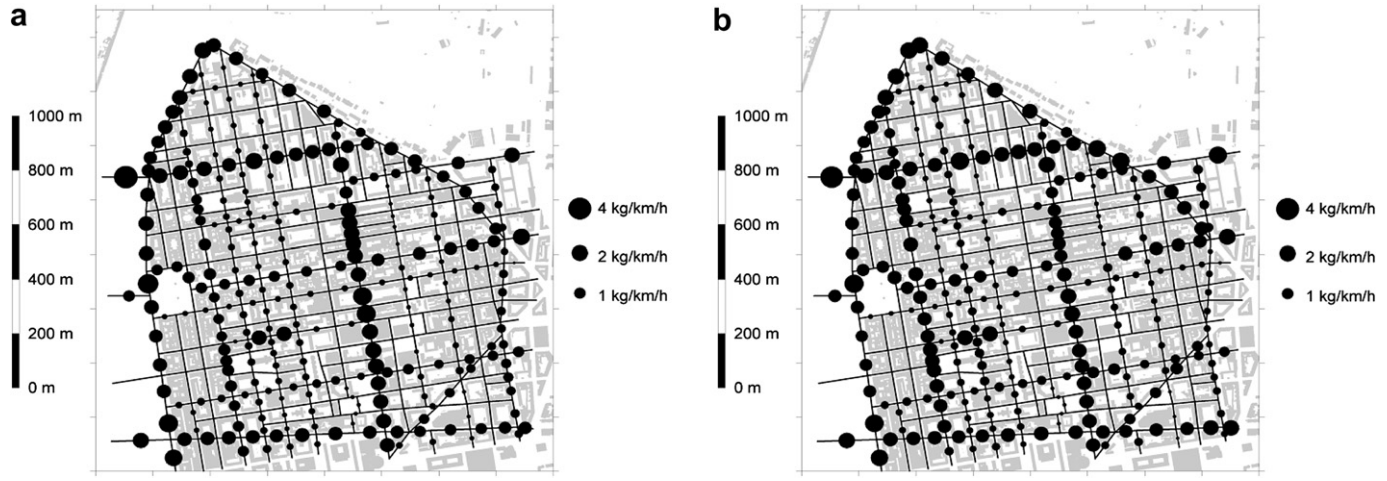

Fig. 10. Cartography of NO_X emissions (equivalent NO_2). a) Morning rush hour; b) Evening rush hour.

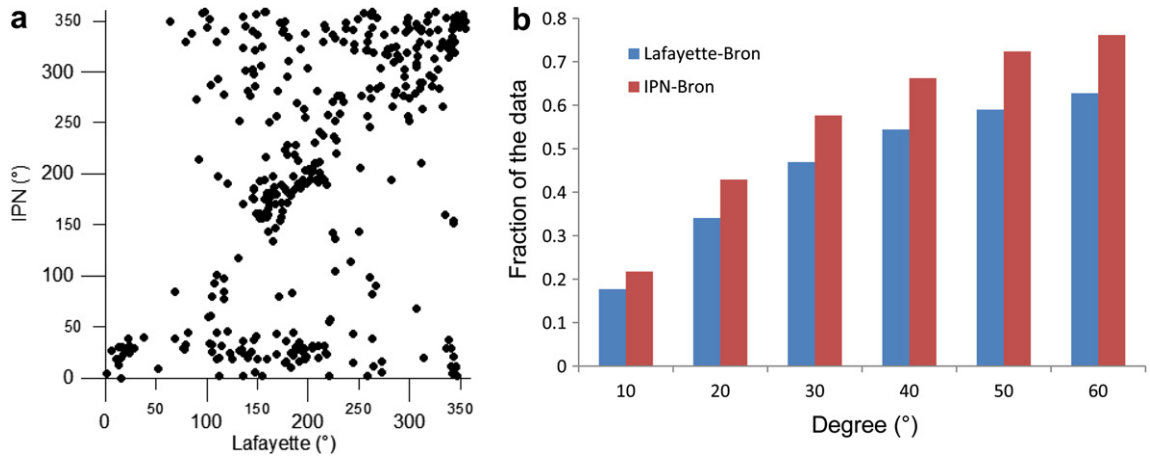

Fig. 12. Wid direction data analysis. a) Correlation between wind direction measuraments in the two urban meteorological stations. b) Difference between Bron airport data urban stations data: percentage of data within an error of 10, 20, 30, 40, 50 and 60°.

be negligible. However, possible wind direction deviations between the sub-urban and the urban sites could not be quantified, given the high scatter registered between the three data sets. As Fig. 12-b shows, this scatter produces significant differences between the wind directions measured at Bron airport and that registered by the two urban stations.

3.4. Background pollution

SIRANE provides pollutant concentrations due only to pollutants emitted within the studied domain. Therefore, in order to compare the SIRANE outputs with in-situ measurements it is necessary to take into account the contribution due to background pollution. If we consider nitrogen oxides, which are involved in chemical reactions in the atmosphere, background concentration of ozone also have to be retained.

In this study we have used background values for nitrogen oxides and ozone measured by monitoring station located outside the studied district (cf. Fig. 1): Croix-Luizet, Gerland and Saint-Just. Since the background pollution levels depend on pollutant sources located upwind of the domain it is advantageous to adopt different reference stations depending on the wind direction. However, a comparison between the statistics of the time series collected at the three different sites show little differences (Fig. 14). Therefore we assumed that the reference background level was given by the mean of the three concentration levels (Fig. 14).

No hourly background level was available for BTX concentrations, which were only measured by the monitoring station placed in rue Garibaldi, a busy street canyon within the studied district. We could however refer to background levels averaged over 15 days, measured by PDT placed outside of the district expressly for the LYON6 campaign. Since we can reasonably assume BTX to be passive on that time scale, we refer to this averaged value as an estimate for the background level which can be added linearly to the 2 weeks averaged concentrations computed by SIRANE (the same procedure cannot be applied to reactive compounds such as NO_X). Background BTX concentrations are given in Table 7.

Table 6
Characteristics of the measurement site.

Parametre	Bron	Lafayette	IPN
Measurement height	10 m	31.5 m	24 m
Aerodynamic roughness	0.1 m	0.9 m	0.9 m
Displacement height	0 m	13 m	13 m
Mean wind velocity	2.90 m s^{-1}	1.39 m s^{-1}	1.42 m s^{-1}

3.5. General input parameters for SIRANE

Other than emissions, meteorology and background pollution, SIRANE requires a series of other physical parameters as input data. These are listed in Table 8.

The latitude of the site is used to compute the solar elevation. This parameter, together with the albedo, the emissivity and Priestley–Taylor coefficient, is needed to compute the energy balance at ground level and therefore the sensible heat flux between the ground and the atmosphere (Soulhac et al., 2011). Albedo and emissivity were estimated from the land use cover CORINE (Carissimo et al., 1995). We assumed a value 0.5 for the Priestley–Taylor coefficient, as suggested by Hanna and Chang (1992) for an urban environment.

The aerodynamic roughness and the displacement height of the district, used by the meteorological pre-processor to compute the vertical profile of mean horizontal velocity over the district, were determined according to the method suggest by MacDonald et al. (1998), as a function of porosity factors, namely the density λ_P, and the frontal density λ_F of the group of obstacles. The general dependence of the roughness length z_0 and of the displacement height d on λ_P and λ_F adopted here is that proposed by MacDonald et al. (1998):

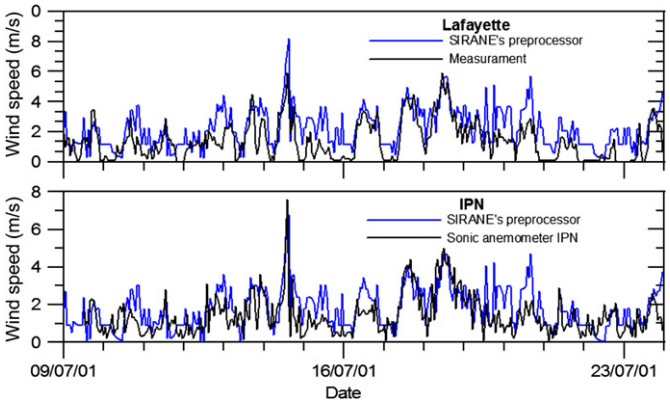

Fig. 13. Comparison of temporal evolution of wind speed measured by urban stations and simulated by the meteorological pre-processor of SIRANE.

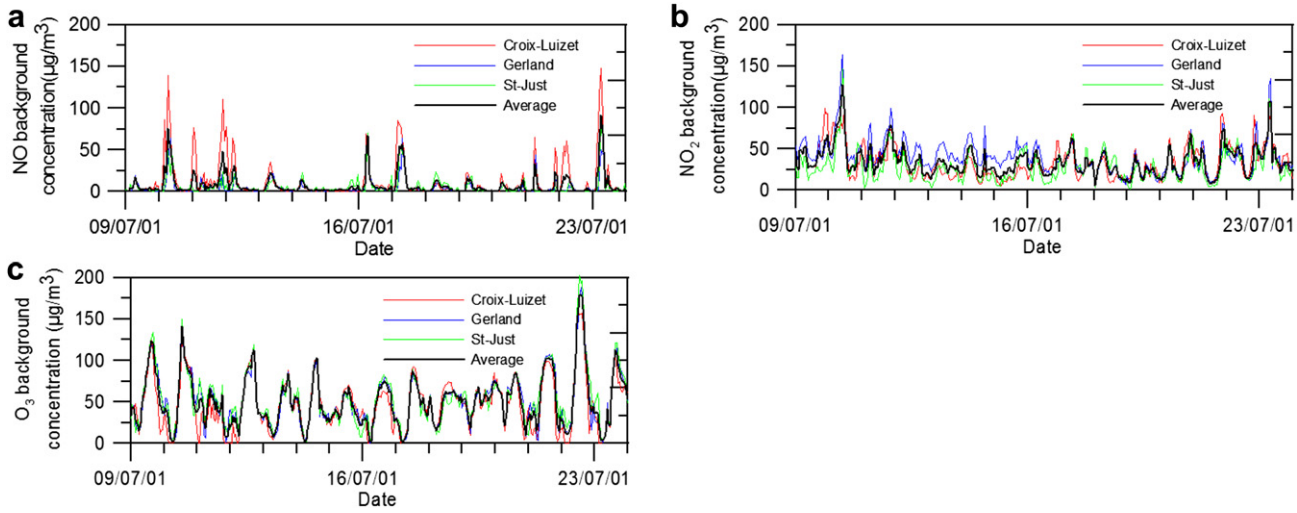

Fig. 14. Temporal evolution of nitrogen oxyde and ozone concentrations. a) NO background concentration; b) NO_2 background concentration; c) Ozone background concentration.

$$\begin{cases} \dfrac{d}{H} = 1 + \alpha^{-\lambda_P}(\lambda_P - 1) \\ \dfrac{z_0}{H} = \left(1 - \dfrac{d}{H}\right)\exp\left[-\left(\dfrac{1}{2}\beta\dfrac{C_{D,\text{build}}}{\kappa^2}\left(1 - \dfrac{d}{H}\right)\lambda_F\right)^{-1/2}\right] \end{cases} \quad (4)$$

where $C_{D,\text{build}}$ represents the drag coefficient of an individual obstacle ($C_{D,\text{build}} \sim 1.2$) and α and β are constants. Their values are assumed here to be $\alpha = 4.43$ and $\beta = 1$, as suggested in case of staggered cubical obstacles. From GIS data we could estimate the mean obstacle height as equal to 20 m and the porosity parameters $\lambda_P = 0.38$ and $\lambda_F = 0.18$. With these values we obtain a displacement height $d = 13$ m and a district roughness length $Z_{0,\text{district}} = 0.9$ m.

The minimal value of the Monin–Obukhov height $L_{\text{MO,min}}$ avoids highly stable stratifications, which rarely occur in urban areas since the shear generated turbulence and the anthropogenic fluxes are generally high. We assume $L_{\text{MO,min}} = 100\ z_0$, as suggested by De Haan (1999). The NO_2 rate is fixed at 10% and is used to determine the ratio of NO_2/NO_X at the emission. In the present study, the ratio of the reaction constant k_1/k_3 of the Chapman cycle (Soulhac et al., 2011) is assumed to be constant in time, uniform over the whole domain and equal to 20 ppb. It is worth mentioning that the chemical module is activated only to compute NO, NO_2 and O_3 concentrations whereas BTX are assumed as passive contaminants.

Finally, the wash out rate is needed to estimate the wet deposition of pollutant, depending on the intensity of the precipitation. The values of the wet deposition model constants a and b of are given by literature data (Slinn, 1984).

4. Comparisons between in-situ measurements and numerical results

SIRANE has been run on the scenario defined in § 2. Numerical simulations were performed over 15 days, from9–24th July 2001.

Table 7
Background BTX concentration (averaged over 15 days).

Pollutant	Background level
Benzene	1.18 µg m^{-3}
Toluene	3.85 µg m^{-3}
mp-Xylem	1.71 µg m^{-3}
o-Xylem	Not available

As specified in part I of this study (Soulhac et al., 2011) SIRANE assumes a quasi-steady approximation, therefore describing the temporal evolution of all variables (emissions, meteorology, background level) as the succession of stationary conditions. The hourly concentrations computed by SIRANE provide a data set which can be compared with the time series of hourly concentrations measured by the monitoring stations (§ 4.2) and with the 15 day averages provided by the PDT (§ 4.1). Following Chang and Hanna (2004), the differences between experimental and numerical values have been quantified by means of the fractional bias FB, the relative error ER (defined in § 3.2.1) and of the following statistical indices:

- The normal mean square error: $\text{NMSE} = \dfrac{\overline{(C_p - C_m)^2}}{\overline{C_p}\,\overline{C_m}}$.
- Correlation coefficient: $R = \dfrac{\overline{(C_p - \overline{C_p})(C_m - \overline{C_m})}}{\sqrt{\overline{(C_p - \overline{C_p})^2}\,\overline{(C_m - \overline{C_m})^2}}}$
- The mean geometrical bias: $\text{MG} = \exp[\overline{\ln(C_p)} - \overline{\ln(C_m)}]$
- The geometrical mean squared variance: $\text{VG} = \exp[\overline{(\ln(C_p) - \ln(C_m))^2}]$.
- The "fraction in a factor of 2": fraction FAC2 of the data for which $0.5 \le C_p/C_m \le 2$.

where C_p and C_m are the measured and modelled quantities respectively. Following Chang and Hanna (2004) and Chang et al.

Table 8
General input parameters for SIRANE.

Latitude	45.598°
District aerodynamic roughess	0.9 m
Displacement height	13 m
Mean buildings height	20 m
Aerodynamic roughness of building walls	0.05 m
Albedo	0.19
Emissivity	0.88
Priestley–Taylor coefficient	0.5
Wind measurement height	10 m
Aerodynamic roughness of the measurement site	0.1 m
Displacement height of the measurement site	0 m
Minimal Monin–Obukhov height	90 m
NO_2 emission rate	10%
Reaction constant ratio k_1/k_3	20 ppb
Wash out rate Λ (s^{-1}), as a function of the intensity precipitation P (mm/h)	$\Lambda = a\,P^b$ with $a = 10^{-4}$ h mm^{-1} s^{-1} $b = 1$

(2005) the performances of a model can be defined as 'good' when the following criteria are satisfied: $-0.3 \leq FB \leq 0.3$, $\sqrt{NMSE} \leq 2$, $0.7 \leq MG \leq 1.3$, $VG \leq 1.6$, $FAC2 \geq 0.5$.

4.1. Averaged concentration over 15 days

The comparison between SIRANE outputs and 15 days averages was performed referring to passive tube measurements. As discussed in § 2.3, we have applied a corrective factor of 0.69 to the PDT measurements (this value corresponds to the slope of the linear regression of the data presented in Fig. 5). Comparison between SIRANE and corrected concentrations of NO_2 and BTX are presented in Fig. 15 and Table 9.

The results show that, according to Chang and Hanna criteria (1994), the SIRANE performances are 'good' in simulating the spatial distribution of NO_2 and Benzene observed experimentally. The best performances are achieved for NO_2 with a very low (about 0.01) fractional bias (FB) and mean error (ER = 0.13). Furthermore the optimal value of FAC2 shows that the ratio between the modelled and the experimental values is less than 2 in all cases.

Comparisons of the other BTX concentrations are less satisfactory. We notice that the sign of the FB is positive for benzene and negative for all other BTX. This means that the ratio between benzene concentrations and concentration of other BTX is significantly different between model and measurements. Since all BTX can be reasonably considered as passive scalars, the ratio of the simulated concentrations must be equivalent to that imposed at the source, which is fixed by the COPERT III methodology. However, the measured concentrations show that this is not the case. This anomaly is evidenced in Table 10, where we compare the values of these ratio provided by COPERT III and those derived by the measurements. It is worth mentioning that these ratios were obtained by subtracting the background values of BTX to the direct measurements provided by passive tubes and monitoring stations placed within the district. The experimental values in Table 10 clearly show that, in accordance with our simulations, the COPERT III methodology highly underestimates the ratios o-Xylem/Benzene, Toluene/Benzene and especially the ratio mp-Xylem/Benzene. Comparisons performed in other studies (Bravo et al., 2002) have shown experimental results similar to those obtained in the present study, with a measured ratio of Toluene/Benzene between 3 and 5. We have therefore to conclude the matrix species repartition provided by COPERT III is not coherent with the measured values. A correction of the elements of this matrix is then needed in order to improve the performances of the modelling chain.

Table 9
Parameters used for the comparison between SIRANE and the diffusion tubes measurements. Results that do not respect Chang and Hanna (2004) criteria for a 'good' model are in bold italic.

	NO_2	Benzene	Toluene	mp-Xylem	o-Xylem
FB	0.01	0.19	***−0.41***	***−0.87***	***−0.37***
$\sqrt{NMSE}$	0.16	0.53	0.64	1.16	0.74
ER	0.13	0.44	0.46	0.82	0.51
R	0.69	0.09	−0.07	0.04	0.01
MG	1.02	1.19	***0.65***	***0.40***	***0.65***
VG	1.03	1.32	1.47	***2.97***	***2.21***
FAC2	1.00	0.80	0.70	***0.45***	0.74

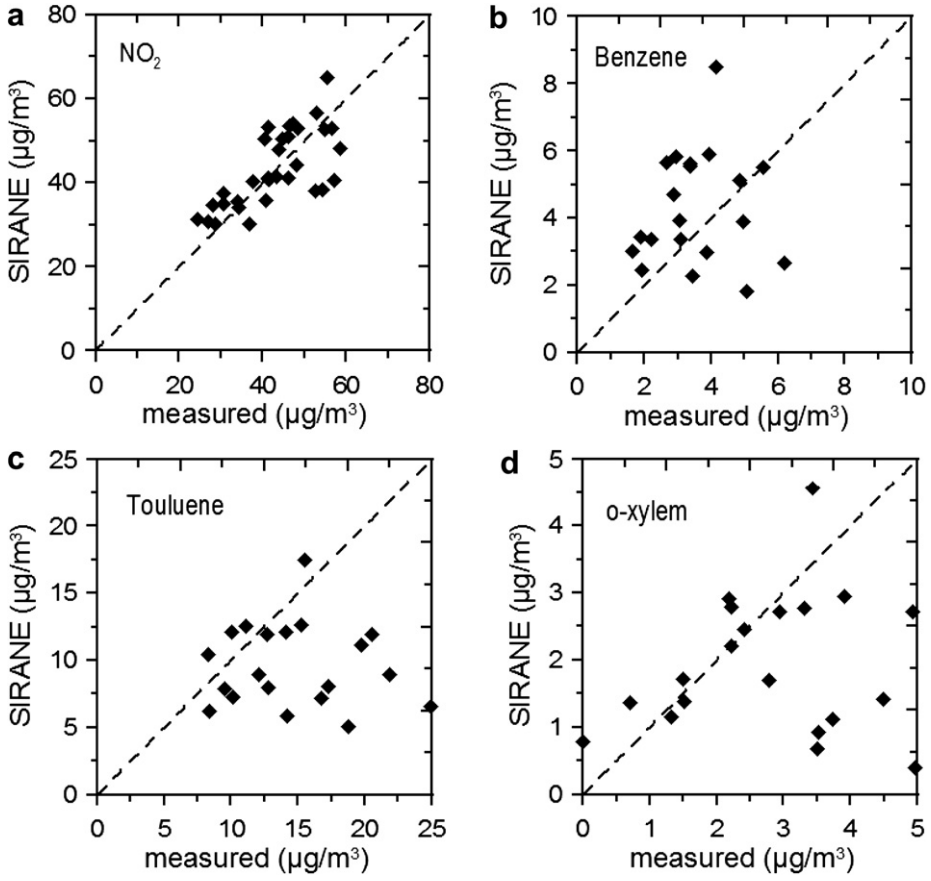

Fig. 15. Comparisons between passive tube measurements and SIRANE outputs. a) Correlation SIRANE-measurements for NO_2. b) Comparison SIRANE-measurements pour le NO_2. c) Comparison SIRANE-measurements for BTX.

Table 10
Ratio between benzene and other BTX, obtained by air concentration measurements and by the speciation matrix provided by COPERT III.

	Diffusion tubes	Monitoring stations	COPERT III Conventional Fuel Veh.	COPERT III Fuel Veh post Euro I
Toluene/Benzene	4.66	3.79	1.88	1.96
mp-Xylem/Benzene	4.41	3.94	0.98	0.97
o-Xylem/Benzene	1.18	1.12	0.66	0.40

4.2. Concentration time series

Hourly concentrations of NO_X, NO, NO_2, O_3, benzene and toluene computed by SIRANE are compared to those measured by the three monitoring stations. A first analysis of the result is performed by comparing the statistical distribution of the simulated and measured data set regardless of the temporal evolution of the data. As an example we show the Q–Q plots concerning NO_2 concentration for the three reference sites. As Fig. 16 shows, the general accordance of the simulated and measured data sets is good, except for few extreme values in Station 2, where the model tends to underestimate field data, and Station 3, where the model overestimate the field data.

In order to evaluate more deeply the model performances we have then analysed the concentration time series. The temporal evolution of pollutant concentration is relative to Station 1 is represented in Fig. 17, whereas the statistics of the time series for the three stations are compared in Table 11.

The best model performances are those related to NO_2 results, with statistical indices that respect all Hanna and Chang criteria for the three stations. It is worth noting that these performances are slightly better to those related to NO_X concentrations. The relative error for NO_X varies between 0.33 and 0.53, which is relatively high, and the FB and the VG in Station 3 are beyond the Chang and Hanna criteria. This uncertainty is partly due to the uncertainties of the traffic scenario (§ 3.2.1), partly to errors of the emission model and to the parametrisation implemented in SIRANE. However, the better performances on NO_2 than NO_X suggest that the implemented photochemical model (Soulhac et al., 2011), which assumes photo stationary conditions and a constant photolysis rate, introduces a correction to those errors. This correction improves the model performance for NO_2 and at the same time worsens the model prediction for NO, which turns out to be the chemical species with the worst scores. The model performances on O_3 are 'good' for Station 2 and 3, whereas in Station 1 the values of FB, MG and VG slightly exceed the limits of Chang and Hanna criteria. Station 1 is the only placed within a street with high vehicular pollutant sources in it, where we the photochemical conditions are therefore expected to be far from a stationary condition. This can explain the worse model performance for O_3 in Station 1 compared to the two other stations. These results on secondary pollutants show the importance of a reliable photochemical model in the model prediction. We believe that these topics deserve further detailed studies.

Finally we focus on BTX. Results for Benzene in Station 1 show the statistical parameters are within the Hanna and Chang criteria except for the VG. This confirms the ability of the model in simulating well passive scalar dispersion. Results for Toluene are significantly worse with a low value of FAC2 = 0.37 and an FB = −0.67 which indicates a systematic underestimation of the model. As mentioned in the previous paragraph this feature can be attributed to a significant error in the ratio Toluene/Benzene in the emissions data which turns out to be underestimated by the COPERT III model.

5. Sensitivity study

The goal of the sensitivity study is to estimate the influence of the modification of different input parameters on the concentration outputs of SIRANE. To quantify these influences, we refer to three time and spatially averaged parameters:

- $C_{NO_{X,dir}}$ represents concentrations of NO_X averaged over 15 days and over all streets of the district, without taking background pollution into account. This parameter allows us to estimate the direct influence of a parameter on the concentration of a passive tracer.
- C_{NO_X} represents concentrations of NO_X averaged over 15 days and over all streets of the district, taking background pollution into account. This parameter allows us to estimate the relative influence of a parameter on the total concentration of a passive tracer.
- C_{NO_2} represents concentrations of NO_2 averaged over 15 days and over all streets of the district, taking background pollution into account. This parameter allows us to estimate the influence of an input parameter on the chemical transformation of the Chapman cycle.

It is worth mentioning that the LYON6 campaign showed the significant contribution of background concentration to pollution levels within the studied district. The values of $C_{NO_{X,dir}}$ and C_{NO_X} for the two reference case are 36.36 μg m^{-3} and 82.79 μg m^{-3} respectively. This means that the background level corresponds on average (over time and space) to about 56% of the total concentration whereas the direct contribution simulated by the model represents only 44%. For this reason we have adopted two different parameters, $C_{NO_{X,dir}}$ and C_{NO_X}, to evaluate the influence of the input

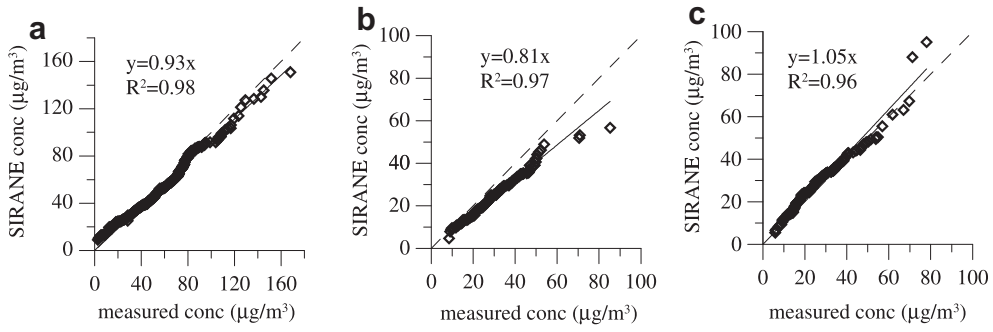

Fig. 16. Comparison by Q–Q plot of the simulated and measured NO_2 concentration data set for the a) Station 1, b) Station 2 and c) Station 3.

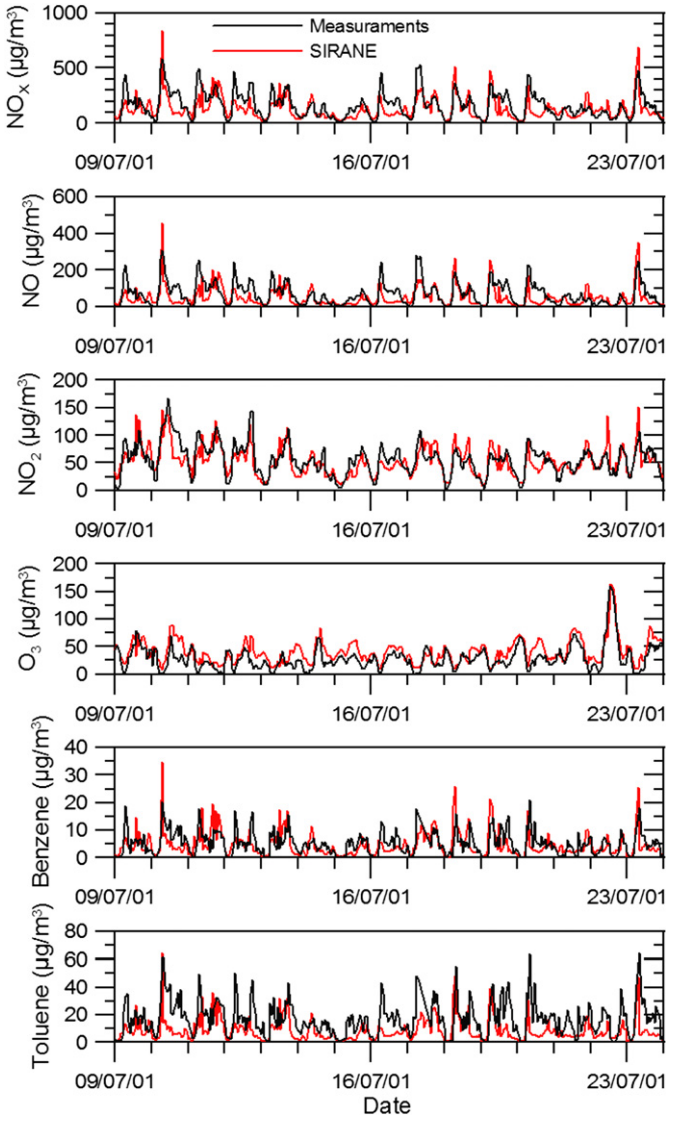

Fig. 17. Comparison of the temporal evolution of pollutant concentrations measured by the monitoring Station 2 (a) and 3 (b) computed by SIRANE.

data. This high background concentration level will be crucial in explaining the relative importance of the different parameters on the concentration outputs.

The sensitivity analysis presented here only concerns the influence of varying input parameters on the model output and does not include the analysis of the parametrisations adopted in SIRANE. We indeed expect that variations in the estimates of the wind speed along the street axes, referred as U_{street}, or in the vertical mass exchange velocity u_d between the urban canopy and the atmosphere can alter significantly the results. The accuracy of the parametric model has been analysed in specific studies by means of wind tunnel experiments (Garbero, 2008; Carpentieri et al., 2009), that allowed us to eliminate all incertitude on source intensity and position as well as those related to the velocity field within and above the simulated urban canopy.

In what follows we analyse the influence of the input parameters related to three main features, emissions, meteorology and geometry. The sensitivity analysis has been performed in two steps. Firstly we vary the input values of all parameters by 50% in order to identify the one that induce the highest variation on the model outputs. Secondly, we evaluate more carefully the influence of these parameters by performing a differential sensitivity analysis (Fig. 18).

In the analysis we include also the effect of varying scenarios obtained by altering input values of the whole modelling chain, such as the traffic fluxes and the composition of the vehicular fleet.

5.1. Traffic and emission data

The influence the pollutant emission factor on the model outputs is shown in Fig. 18-a, where we have plotted the variations of $C_{NO_{X,dir}}$, C_{NO_X} and C_{NO_2} depending on variation of the pollutant emissions E. Both of them are plotted normalised by their reference values C_0 and E_0 of the base scenario. The linearity of the mathematical model implies that a modification of 50% of the emission rates induce a variation of 50% in the direct concentration $C_{NO_{X,dir}}$. However, if we take into account also the contribution of background pollution, the modification decreases to 22%, whereas if we take into account chemical transformation on NO_2, concentrations drop to 15%.

As expected, the influence of emission rates on concentration is significant. To go further with the analysis and test the different steps of the modelling chain, we focus on the different parameters that determine the emission rates: the traffic intensity, the vehicular fleet distribution and the emission factors. The influence of traffic and emission factor on the parameters $C_{NO_{X,dir}}$, C_{NO_X} and C_{NO_2} is summarised in Table 12.

Firstly, we tested the influence of traffic intensity by varying traffic fluxes of 50% in all streets of the district. This entrains a modification in pollutant concentrations that exceed 50% on the direct concentration $C_{NO_{X,dir}}$. This is due to the fact that the variation in traffic fluxes induces a variation in speed of vehicles too and therefore on the emission rates, amplifying the effect on pollutant emission of nitrogen dioxides. Taking into account background concentrations, the impact on output NO_X concentration is about 25%. This value is further decreased taking into account chemical transformation on NO_2 levels.

The composition of the vehicular fleet mainly depends on the year taken as a reference, since it depends on the evolution of emissions regulation policies and on the renewal of the vehicular

Table 11
Comparison between SIRANE outputs and measurement. Results that do not respect Chang and Hanna (2004) criteria for a 'good' model are in bold italic.

	Station 1						Station 2				Station 3			
	NO_X	NO	NO_2	O_3	Benzene	Toluene	NO_X	NO	NO_2	O_3	NO_X	NO	NO_2	O_3
FB	−0.21	***−0.33***	−0.05	***0.33***	−0.18	***−0.67***	0.20	***0.80***	−0.20	−0.22	***0.49***	***1.15***	0.07	0.05
$\sqrt{NMSE}$	0.58	0.72	0.34	0.43	0.81	1.02	0.46	0.90	0.39	0.37	0.59	1.32	0.30	0.14
ER	0.53	0.74	0.30	0.54	0.68	0.82	0.33	1.02	0.30	0.28	0.49	1.26	0.27	0.20
R	0.66	0.63	0.76	0.84	0.47	0.48	0.73	0.70	0.66	0.83	0.86	0.72	0.81	0.97
MG	0.90	0.86	1.00	***1.75***	0.98	0.51	1.24	***3.47***	0.82	0.79	1.65	***6.02***	1.11	1.18
VG	1.61	***2.92***	1.18	***2.26***	2.77	***3.66***	1.20	***9.14***	1.15	1.13	1.45	***80.16***	1.12	1.26
FAC2	0.68	***0.44***	0.91	0.71	0.53	***0.38***	0.90	***0.26***	0.94	0.96	0.72	***0.16***	0.97	0.93

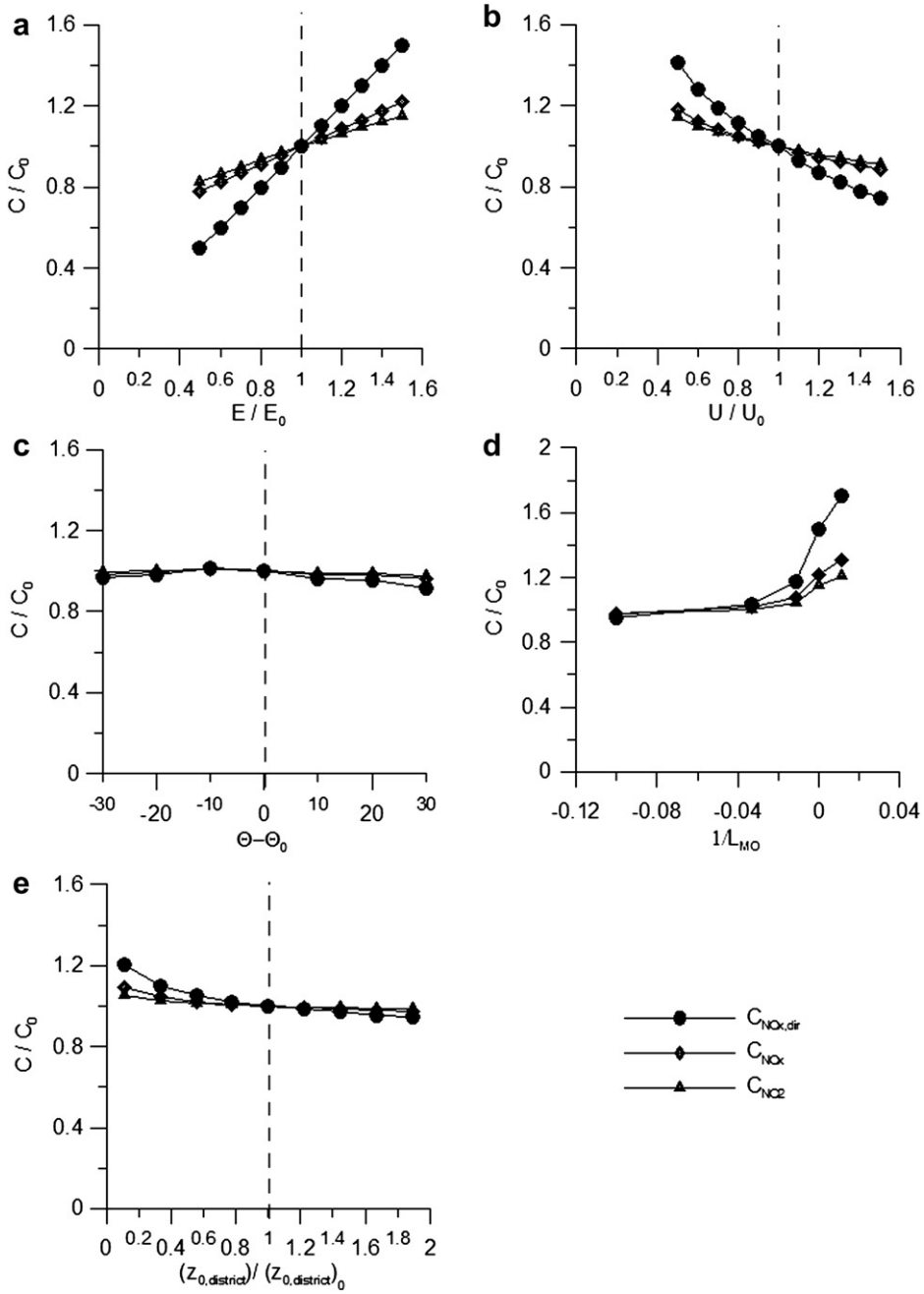

Fig. 18. Differential sensitivity analysis on a) vehicles pollutant emissions E, b) wind velocity U, c) wind direction, d) Monin-Obhukov length, e) district urban roughness $Z_{0,district}$. The values C_0, E_0, U_o, Θ_o, and $(Z_{0,district})_0$ refer to the base scenario.

Table 12
Sensitivity of SIRANE to traffic emission data.

	Emissions +50%	Emissions −50%	Traffic +50%	Traffic −50%	Vehicular fleet 1999	Vehicular fleet 2003	NO_2/NO_x at emission +50% (=0.15)	NO_2/NO_x at emission −50% (=0.05)
Relative variation $C_{NO_{x,dir}}$	+50%	−50%	+59.33%	−51.70%	+15.99%	−15.22%	0%	0%
Relative variation C_{NO_x}	+21.96%	−21.96%	+26.06%	−22.71%	+7.02%	−6.68%	0%	0%
Relative variation C_{NO_2}	+14.22%	−16.60%	+16.75%	−17.29%	+4.76%	−4.75%	−2.15%	+2.11%

fleet. The reference data set by the ADEME (Bourdeau, 1997) provide the annual evolution of the fleet until 2020. In the present study we adopted the information for the year 2001, and we compared the results with those obtained with the data set for 1999 and a data set for 2003. The direct concentration $C_{NO_{X,dir}}$ varies by about 15%, whereas the variations of C_{NO_X} and C_{NO_2} do not exceed 7%. This variation is significant, if we consider that it is due to modifications in the vehicular fleet occurring over 2 years only.

Finally we tested the effects of variations of the NO_2 emission rate factor. This parameter defines the ratio NO_2/NO_x in the emissions of nitrogen oxides. This factor does not affect the parameters of $C_{NO_{X,dir}}$ and C_{NO_X}, which are related to the concentrations of NO_X that is considered as a passive tracer. The variation of 50% of this factor (which induce variations between 0.05 and 0.15, that represent a range of realistic variations) on NO_2 concentration is of about 2%, which is relatively slight compared to the variations induced by the other parameters. This is partly due to the non linearity of the chemical reactions, which damp the effects on the variation of this parameter. Conversely, if we focus on VOC/BTX, which are considered as passive tracers and whose background values are lower than those of other chemical species, we notice that the emission rate factor has a greater influence on the model outputs.

Summarising, the impact of the intensity of the emission rates on the concentration simulated by SIRANE is significant. Therefore, the parameters controlling this intensity highly affect the quality of the results. In particular the results show high sensitivity on the composition of the vehicular fleet. The influence of the pollutant speciation (NO_2 rate factor or COV/BTX speciation) on the level of background pollution and on chemical transformation varies for each pollutant species (higher for BTX than for NO_2).

5.2. Meteorological data

The results of the sensitivity study for the main meteorological parameters are summarised in Table 13. For all tested parameters (except for the ground level temperature whose effect is negligible), the influence on the direct concentration $C_{NO_{X,dir}}$ is always greater than that computed for the two other parameters C_{NO_X} and C_{NO_2}. For this reason, in what follows, we will mainly consider the influence of the direct concentration $C_{NO_{X,dir}}$.

The most influent meteorological parameter is the wind velocity (Fig. 18-b and Table 13). An increase of 50% in wind velocities induces a decrease in pollutant concentration of about 26% whereas a decrease in wind speed of 50% induce an increase in pollutant concentration of 42%. This dissymmetry is due to the fact that a variation in wind speed entrains also variation in turbulence intensities and stability parameters and therefore on parameters characterising the pollutant dispersion.

As mentioned in § 3.3 the wind direction is the parameter which is determined with the highest level of uncertainty. We have therefore analysed the effect of a systematic deviation of the wind direction compared to that measured at the Bron Airport. The results, presented in Fig. 18-c, show that these deviation have very little effect on the spatially averaged parameters that have been adopted as indicators of the model performances. Of course, we would expect a much higher effect on comparison performed on a single fixed point. Such a sensitivity study however would require further detailed analyses both on the position of the single receptor within the district and of its position within the single street canyon. Both aspects are beyond the scope of this paper.

We have then studied the influence of a modification of 5 °C of ground level temperature. This parameter is taken into account to estimate the stability condition and to compute the molar volume

Table 13
Sensitivity of SIRANE to meteorological data.

	Wind speed +50%	Wind speed −50%	Temperature +5 °C	Temperature −5 °C	Cloud coverage = 0 octas	Cloud coverage = 8 octas	Simulation performed in january	Priestley −Taylor coeff. = 0	Priestley −Taylor coeff. = 1	L_{MO} minimal = 50 m	L_{MO} minimal = 150 m
Relative Var. of $C_{NO_{X,dir}}$	−25.81%	+41.60%	+0.06%	+0.13%	+0.61%	+9.25%	+43.02%	−5.35%	+14.73%	+1.84%	−1.86%
Relative Var. of C_{NO_X}	−11.34%	+18.27%	+0.03%	+0.06%	+0.27%	+4.06%	+18.89%	−2.35%	+6.47%	+0.81%	−0.82%
Relative Var. of C_{NO_2}	−8.41%	+13.53%	+0.46%	−0.44%	+0.16%	+2.60%	+9.80%	−1.59%	+3.97%	+0.49%	−0.49%

of pollutant species involved in chemical reactions. Table 13 shows that the influence of ground level temperature is almost negligible.

In this study, all information on thermal fluxes between the ground and the atmosphere has been computed from cloud coverage estimates. Cloud coverage can have opposing effects on thermal fluxes between soil and atmosphere. During the day, clouds limit the solar radiation received by the earth's surface and therefore the flux of sensible heat from the ground to the atmosphere. During the night the clouds limit the cooling of earth surface and soften the stability of the atmospheric boundary layer. The average effect of a modification of the values of the cloud coverage is therefore difficult to predict. During the LYON6 campaign, the mean measured cloud coverage was 4.9 octas (0 = clear sky; 8 = completely covered sky). In the sensitivity analysis we have tested two extreme situations: a condition of clear sky for the whole simulation period and a condition of completely covered sky. The modifications on the direct concentration $C_{NO_{X,dir}}$ is 1% for a clear sky and 9% for the cloudy condition. The effect of a continuously cloudy sky induces stability conditions that attain the neutral stratification. Since the simulation period is in summer, the atmospheric conditions are mainly unstable. Therefore, the effect of this artificially imposed cloud coverage has been to induce higher ground level concentrations. The previous results have shown the influence of atmospheric stability on ground level concentrations. The stability conditions are influenced by the solar radiation which depends on cloud coverage, and on the hour, the day and the month considered. To show the influence of these latter parameter we have simulated the LYON6 campaign as if it took place in January instead of July, and keeping unaltered all other input parameters. Results shown that this induce an increase on the direct concentration $C_{NO_{X,dir}}$ of 43%.

The Priestley–Taylor coefficient quantifies the water vapour at ground level that can evaporate. A value of 0 corresponds to a completely dry soil whereas a value of 1 indicates a soil saturated with water. The value adopted in the reference simulation was 0.5. We have then tested the influence of this parameter by imposing the two limiting values 0 and 1, which modifies the direct concentration $C_{NO_{X,dir}}$ between 5 and 15%. This can be explained by the influence of this parameter on the atmospheric stability and therefore on pollutant dispersion. As the Priestley–Taylor coefficient is reduced the flux of latent heat is reduced. This implies an increase of the sensible heat flux, which acts directly on the thermal stratification of the atmosphere. Conversely, as the coefficient is increased, the latent flux rises, the sensible flux decrease, the atmosphere is less unstable and the dispersion of pollutant reduced.

The sensitivity analysis on the Monin–Obukhov length has been conducted in two different ways. One concerns the values of the minimal Monin–Obukhov length adopted by the model. The second focuses on the effect of a simulated forced stability conditions over the whole campaign duration. A minimal value of the Monin–Obukhov length was introduced in SIRANE to avoid too stable and unrealistic atmosphere above the urban district. The value of this parameter in the reference simulation was 90 m. When this value is reduced, the direct concentration tends to increase as more stable conditions take place. The inverse effect is observed when the value of the minimal L_{MO} is increased. The variations in ground level concentration are slight, less than 2%, because this parameter acts on computations only during the night time, when the direct pollution is almost negligible. However, in case of highly stable condition during the day, this parameter may have a great influence on the results. We have also tested the effect of forced stable and unstable conditions during the 15 days period by assigning a fixed Monin–Obhukov length value. Five different cases have been tested. Three of these concern unstable conditions of varying intensity (L_{MO} equal to −10, −30 and −90), one neutral conditions ($L_{MO} = \infty$) and one stable conditions ($L_{MO} = 90$). The results are presented in Fig. 18-d, where normalized concentration are plotted against the inverse of L_{MO}. As expected the main differences are induced by the neutral and stable conditions which represent a significant forcing with respect to the typical stability conditions observed in the first two weeks of July, when the campaign took place.

Finally we focus on the influence of the precipitation intensity. In SIRANE, the effect of precipitations is taken into account at two levels:

- Precipitations induce wet deposition of pollutant and tend therefore to decrease ground level concentrations.
- As it rains, the Priestley–Taylor coefficient is 1. As shown previously, this value induces more stable atmospheric conditions. It is worth mentioning that this effect is independent on the intensity of the precipitations.

We have investigated the combined influence of these two effects. To that end we focused on two days, the July 14–15th 2001, which were both rainy days. We compared the results for the three output parameters $C_{NO_{X,dir}}$, C_{NO_X} and C_{NO_2}, computed with and without precipitations. Results presented in Table 14 show that the influence of precipitations is to slightly increase ground level concentration. This suggests that, in this case, the effect of increased stability conditions induced by a higher Priestley–Taylor coefficient is higher than that induced by the wet deposition of pollutants.

5.3. Geometrical parameters of the district

To define the street network geometry in SIRANE we can use directly the information provided by the GIS data set on height, width and length of the streets, which are generally known with a high degree of accuracy. Conversely, no direct information is available on the two aerodynamic roughness coefficients needed as input data. These are the roughness of the whole district, referred to as $z_{0,district}$, and the roughness of building walls, referred to as $z_{0,build}$. The former is estimated by mean of morphometric relations (§ 3.5), as proposed by MacDonald et al. (1998), and is used to model the vertical profile of mean velocity. The latter is used to compute the averaged velocity within street canyons. SIRANE adopts a default value of 0.05 m for $Z_{0,build}$. Generally speaking, the aerodynamic roughness coefficient has two opposing effects on pollutant concentrations:

- Lower roughness implies higher wind speed at ground level that tends to decrease concentrations.
- Lower roughness implies lower turbulence level which induces increased concentrations.

Since an error in the estimate of these parameters can affect the results provided by SIRANE we have performed a sensitivity analysis. Results are given in Table 15 and Fig. 18-e. These show that the

Table 14
Sensitivity of SIRANE to wet deposition.

	Simulation without precipitations	Simulation with precipitations	Relative variation
$C_{NO_{X,dir}}$	24.16 μg m^{-3}	25.21 μg m^{-3}	+4.33%
C_{NO_X}	54.90 μg m^{-3}	55.95 μg m^{-3}	+1.91%
C_{NO_2}	27.09 μg m^{-3}	27.41 μg m^{-3}	+1.19%

Table 15
Sensitivity of SIRANE to geometrical parameters.

	District Roughness +50%	District Roughness −50%	Building roughness = 0.01 m	Building roughness = 0.1 m
Relative variation of $C_{NO_{x,dir}}$	−3.08%	+6.16%	−0.80%	+2.69%
Relative variation of C_{NO_x}	−1.35%	+2.71%	−0.35%	+1.18%
Relative variation of C_{NO_2}	−0.80%	+1.55%	−0.20%	+0.58%

direct influence of these parameters is relatively low, between 3 and 6% for a variation of 50% of $z_{0,district}$ and between 1 and 3% for a variation of 50% of $z_{0,build}$. This is mainly due to the fact that both parameters appear as an argument of logarithmic functions. We therefore conclude that these parameters have little influence of the model outputs given that the order of magnitude of their value is respected.

6. Conclusions

In this study we have presented a validation of the urban dispersion model SIRANE by means of a field measurement campaign within a district of Lyon. The validation of the model by means of a systematic comparison of its outputs with field data was performed in three steps.

As a first step we defined the simulation scenario by collecting and organising all input data concerning, streets geometry, meteorological data, emission rates and background pollution. Secondly, we compared the results of the model to in-situ measurements from three monitoring stations and 60 passive tubes. The former provided information on the temporal evolution of the concentration levels whereas the latter on their spatial distribution. This comparison allows us to draw the following conclusions.

- The background concentrations that represent a significant contribution to local pollution levels.
- SIRANE simulates quite well the spatial distribution of pollutants when compared to 15 day averages of NO_2 and benzene.
- The temporal evolution of NO_x, NO_2 and ozone provided by the three monitoring stations is well simulated by SIRANE. Conversely, results for NO do not meet the reliability standard. These results show the need of further investigations on the effect of different photochemical models in the modelling chain.
- We have observed important differences between the model and experimental results of some BTX species (toluene and xylem), collected both by passive tubes and monitoring stations. A first analysis suggests that these errors may be mainly due to erroneous emissions factor provided by the COPERT III methodology.

Moving from these results, the overall model performance, measured using the Chang and Hanna (2004) criteria can be considered as 'good'.

The third and final step consisted of a sensitivity analysis on the model outputs, performed over most of the input data. This analysis showed that the most influential data are those related to traffic fluxes and emission rate factors, in particular those giving the vehicular fleet. Among the meteorological input parameters, the wind velocity is by far the most influent on model performances. Results also show that the estimate of background concentration is essential, since they represent a significant contribution to local pollution levels. It is worth mentioning that the sensitivity analysis presented here focuses on the effects of the incertitude of the input data on SIRANE performances. Other studies focused on the influence of the parametric model implemented in SIRANE (Garbero, 2008; Carpentieri et al., 2009), namely on the pollutant exchange at roof level, on the exchange at street intersections and on the advection of pollutant along the street axes.

This study shows the importance of an approach based on the application of modelling tools for traffic, emissions and pollutant dispersion. The simulation outputs complement field measurements and enable a greater understanding of air pollution dispersion. SIRANE can therefore be applied to simulate the effect of traffic management strategies, traffic plans and emission reduction policies on the air quality, and may become an important tool for Public Authority decision makers.

Acknowledgements

We acknowledge the Région Rhône-Alpes for its financial support of this study and COPARLY/Atmo-RôneAlpes for its support in organising and managing the LYON6 measurement campaign. The authors would also like to express their gratitude to A. Ezzamel for carefully reading the paper and providing a critical review of its content.

References

Arnold, S.J., ApSimon, H., Barlow, J., Belcher, S., Bell, M., Boddy, J.W., Britter, R., Cheng, H., Clark, R., Colvile, R.N., Dimitroulopoulou, S., Dobre, A., Greally, B., Kaur, S., Knights, A., Lawton, T., Makepeace, A., Martin, D., Neophytou, M., Neville, S., Nieuwenhuijsen, M., Nickless, G., Price, C., Robins, A., Shallcross, D., Simmonds, P., Smalley, R.J., Tate, J., Tomlin, A.S., Wang, H., Walsh, P., 2004. Introduction to the DAPPLE air pollution project. Sci. Total. Environ. 332, 139–153.

Borrego, C., Tchepel, O., Costa, A.M., Amorim, J.H., Miranda, A.I., 2003. Emission and dispersion modelling of Lisbon air quality at local scale. Atmos. Environ. 37, 5197–5205.

Bourdeau, B., 1997. Evolution du parc automobile français entre 1970 and 2020. Thèse de doctorat, Université de Savoie – Chambéry.

Bravo, H., Sosa, R., Sanchez, P., Bueno, E., Gonzales, L., 2002. Concentrations of benzene and toluene in the atmosphere of the southwestern area at the Mexico City Metropolitan Zone. Atmos. Env. 36, 3843–3849.

Campbell, G.W., Steadman, J.R., Stevenson, K., 1994. A survey of nitrogen dioxide concentrations in the United Kingdom using diffusion tubes, July-December 1991. Atmos. Env. 28, 477–486.

Carissimo, B., Dupont, E., Musson-Genon, L., Marchand, O., 1995. Note de principe du code MERCURE version 3.1 EDF-DER, HE-3395007B.

Chang, J.C., Hanna, S.R., 2004. Air quality model performance evaluation. Meteorol. Atmos. Phys. 87, 167–196.

Carpentieri, M., Salizzoni, P., Robins, A., Soulhac, L., 2009. Validation of the neighbourhood scale dispersion model through comparison with wind tunnel data. In: Proceedings of the Conference on Physical Modelling of Flow and Dispersion Phenomena Physmod Conference, Rhode Saint-Genese, Belgium.

Chang, J.C., Hanna, S.R., Boybeyi, Z., Franzese, P., 2005. Use of Salt Lake City URBAN 200 field data to evaluate the urban Hazard prediction Assessment Capability (HPAC) dispersion model. J. Appl.Meteorol. 44 (5), 485–501.

Carruthers, D., Blair, J., Johnson, K., 2003. Validation and Sensitivity of ADMS-Urban for London. Cambridge Environmental Research Consultants. TR0191.

De Haan, P., 1999. Studies on short-range air pollution modeling. Thèse de Doctorat, Swiss Federal Institute of Technology Zurich.

Friedrich, M., 1999. A multi-modal transport model for integrated planning. In: Meersman, H., Van de Voorde, E., Winkelmnas, W. (Eds.), Selected Proceedings from Eight World Conference on Transport Research, vol. 2. Elsevier, Antwerp, Belgium.

Fellendorf, M., Nökel, K., Handke, N., 2000. VISUM-online - traffic management for the EXPO 2000 based on a traffic model. Traffic Technol. Int. Annual 2000, London 2/2000.

Gair, A.J., Penkett, S.A., 1995. The effects of wind speed and turbulence on the performance of diffusion tubes samplers. Atmos. Env. 29-18, 2529–2533.

Garbero, V., 2008. Pollutant dispersion in urban canopy study of the plume behaviour through an obstacle array. PhD thesis, Ecole Centrale de Lyon, France.
Gualtieri, G., 2010. A street canyon model intercomparison in Florence, Italy. Water Air Soil Pollut. 212, 461–482.
Heal, M.R., O'Donoghue, M.A., Cape, J.N., 1999. Overestimation of urban nitrogen dioxide by passive diffusion tubes: a comparative exposure and model study. Atmos. Env. 33, 513–524.
Hanna, S.R., Chang, J.C., 1992. Boundary-layer parametrizations for applied dispersion modeling over urban areas. Boundary-Layer Meteorol. 58, 229–259.
Kakosimos, K.E., Hertel, O., Ketzel, M., Berkowicz, 2011. Operational street model (OSPM) – a review of performed validation studies and future perspectives. Environ. Chem. 7, 485–503.
MacDonald, R.W., Griffiths, R.F., Hall, D.J., 1998. An improved method for the estimation of surface roughness of obstacle arrays. Atmos. Env. 32-11, 1857–1864.
Ntziachristos, L., Samaras, Z., 2000. COPERT III. Computer Programme to Calculate Emissions from Road Transport. Methodology and Emission Factors (Version 2.1). Technical report N° 49. European Environment Agency.
Schatzmann, M., Bächlin, W., Emeis, S., Kühlwein, J., Leitl, B., Müller, W.J., Schlünzen, H., 2005. Development and validation of tools for the implementation of European air quality polici in Germany (Project Valium). Atmos. Chem. Phys. Discuss. 5, 9621–9639.
Slinn, W.G.N., 1984. Precipitation scavenging. In: Atmospheric Science and Power Production NTIS report.
Soulhac, L., 2000. Modélisation de la dispersion atmosphérique à l'intérieur de la canopée urbaine. PhD thesis, Ecole Centrale de Lyon.
Soulhac, L., Mejean, P., Perkins, R.J., 2001. LYON6 – Campagne de mesure de la pollution dans un quartier de Lyon. École Centrale de Lyon – COPARLY.
Soulhac, L., Salizzoni, P., Cierco, F.-X., Perkins, R.J., 2011. The model SIRANE for atmospheric urban pollutant dispersion: Part I, presentation of the model. Atmos. Environ. 45, 7379–7395.
Vardoulakis, S., Fisher, B.E.A., Gonzales-Flesca, N., Pericleous, K., 2002. Model sensitivity and uncertainty analysis using roadside air quality measurements. Atmos. Environ. 36, 2121–2134.
Wood, C.R., Arnold, S.J., Balogun, A.A., Barlow, J.F., Belcher, S., Britter, R.E., Cheng, H., Dobre, A., Lingard, J.J.N., Martin, D., Neophytou, M.K., Petersson, F.K., Robins, A.G., Shallcross, D.E., Smalley, R.J., Tate, J.E., Tomlin, A.S., White, I.R., 2009. Dispersion experiments in Central London: the 2007 DAPPLE project. Bull. Am. Meteorol. Soc. 90, 955–969.